PNAS
www.pnas.org

Supplementary Information for

Inhibition of GCN2 sensitizes ASNS-low cancer cells to asparaginase by disrupting the amino acid response

Akito Nakamura[a,b,1], Tadahiro Nambu[b], Shunsuke Ebara[b], Yuka Hasegawa[b], Kosei Toyoshima[b], Yasuko Tsuchiya[b], Daisuke Tomita[b], Jun Fujimoto[b], Osamu Kurasawa[b], Chisato Takahara[c], Ayumi Ando[c], Ryuichi Nishigaki[c], Yoshinori Satomi[c], Akito Hata[a,d], and Takahito Hara[b]

[a] Oncology Drug Discovery Unit, Takeda Pharmaceuticals International Co., 40 Landsdowne Street, Cambridge, MA 02139, USA
[b] Oncology Drug Discovery Unit, Takeda Pharmaceutical Company Limited, Kanagawa 251-8555, Japan.
[c] Integrated Technology Research Laboratories, Takeda Pharmaceutical Company Limited, Kanagawa 251-8555, Japan.
[d] Bio Molecular Research Laboratories, Takeda Pharmaceutical Company Limited, Kanagawa 251-8555, Japan.

[1] **Corresponding author:** Akito Nakamura
Oncology Drug Discovery Unit, Takeda Pharmaceuticals International Inc., 40 Landsdowne Street, Cambridge, MA 02139, USA
E-mail: akito.nakamura@takeda.com

This PDF file includes:

- Supplementary text
- Figs. S1 to S10
- Tables S1 to S2
- References for SI reference citations

www.pnas.org/cgi/doi/10.1073/pnas.1805523115

Supporting Information Text

Materials and Methods

Compound synthesis

GCN2iA (**2**) was synthesized from compound 1 in a similar manner as that described in the patent (WO 2013110309A1).

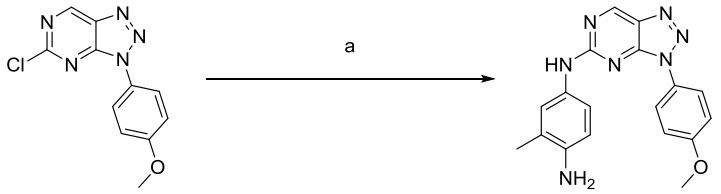

Reagents and conditions: (a) DIEA, 2-methylbenzene-1,4-diamine dihydrochloride, 74%.

N-4-(3-(4-methoxyphenyl)-3*H*-[1,2,3]triazolo[4,5-*d*]pyrimidin-5-yl)-2-methylbenzene-1,4-diamine (**2**). To a mixture of 5-chloro-3-(4-methoxyphenyl)-3*H*-[1,2,3]triazolo[4,5-*d*]pyrimidine (50 mg, 0.19 mmol) in dimethyl sulfoxide (DMSO; 1 mL), 2-methylbenzene-1,4-diamine dihydrochloride (74.6 mg, 0.38 mmol) and diisopropylethylamine (DIEA; 0.167 mL, 0.96 mmol) were added at 25°C. The mixture was stirred at 90°C for 2 h, during which time its color gradually changed to dark brown. The mixture was then poured into saturated $NaHCO_3$ (aq) (20 mL), extracted with ethyl acetate (20 mL), washed with brine, and dried over $MgSO_4$. The filtrate was then concentrated *in vacuo*. The residue was purified by silica gel-column chromatography (*n*-hexane-ethyl acetate = 70:30–0:100) and triturated with iPr_2O. The precipitate was collected by filtration to obtain compound **2** (49.2 mg; 74%) as a pale brown solid. ^{1}H NMR (300 MHz, DMSO-d_6) δ 2.09 (3H, s), 3.86 (3H, s), 4.76 (2H, brs), 6.59 (1H, d, J = 8.5 Hz), 7.16–7.29 (3H, m), 7.54 (1H, brs), 8.05 (2H, d, J = 8.9 Hz), 9.33 (1H, s), and 9.94 (1H, brs).

GCN2iB (**7**) was synthesized as shown in the following scheme:

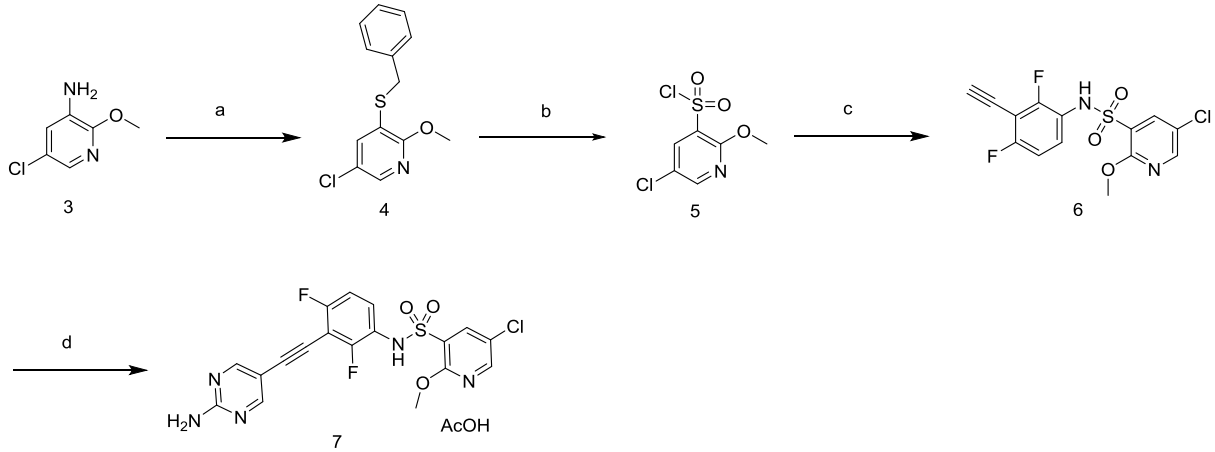

Reagents and conditions: (a) dibenzyldisulfide, pentylnitrite, MeCN; (b) *N*-chlorosucinimide, AcOH, water, 53% (2 steps); (c) 3-ethynyl-2,4-difluoroaniline, pyridine; (d) 1) 2-amino-5-iodopyrimidine, $Pd(PCy_3)_2Cl_2$, Cs_2CO_3, DMSO, 2) recrystallization from DMSO-water-AcOH, 20% (2 steps).

3-(Benzylthio)-5-chloro-2-methoxypyridine (**4**). Pentyl nitrite (8.79 ml, 66.0 mmol) was added dropwise over 20 min to a solution of 1,2-dibenzyldisulfane (8.87 g, 36.0 mmol) and 5-chloro-2-methoxypyridin-3-amine (4.76 g, 30 mmol) in acetonitrile (63.1 mL) at 80°C. The mixture was stirred at 80°C for 30 min and then concentrated *in vacuo*. The residue was purified by silica gel column chromatography (n-hexane-ethyl acetate = 100 : 0-90 : 10) to obtain crude product 4 (5.40 g) as orange oil. This material was used in the next reaction without further purification.

Next, 5-Chloro-2-methoxypyridine-3-sulfonyl chloride (**5**). N-chlorosuccinimide (16.3 g, 123 mmol) was added dropwise for over 10 min to a solution of 4 (5.40 g, 20.3 mmol) in acetic acid (34.9 mL) and water (11.0 mL) at 25°C. The mixture was stirred at room temperature overnight. The mixture was diluted with water, and extracted with EtOAc. The organic layer was washed with brine, dried over $MgSO_4$, and concentrated in vacuo. The mixture was concentrated in vacuo. The residue was purified by silica gel column chromatography (n-hexane-ethyl acetate = 100:0-80:20) to yield 5 (4.40 g, 53% for 2 steps) as orange oil. 1H NMR (300 MHz, DMSO-d6) δ 3.86 (3H, s), 7.91 (1H, d, J = 2.6 Hz), 8.17 (1H, d, J = 2.6 Hz).

5-Chloro-N-(3-ethynyl-2,4-difluorophenyl)-2-methoxypyridine-3-sulfonamide (**6**). The mixture of 3-ethynyl-2,4-difluoroaniline (Ref; 1) (2.78 g, 18.18 mmol), 5 (4.40 g, 18.2 mmol) and pyridine (43.1 g, 545 mmol) was stirred at room temperature overnight. Then, MeOH (10 mL) was added to the mixture, and the mixture was stirred at room temperature for 10 min. The mixture was concentrated *in vacuo*. The residue was purified by silica gel column chromatography (n-hexane-ethyl acetate = 100:0-50:50) to give crude 6 (5.02 g) as beige solid. This material was used in the next reaction without further purification.

N-(3-((2-aminopyrimidin-5-yl)ethynyl)-2,4-difluorophenyl)-5-chloro-2-methoxypyridine-3-sulfon amide acetic acid salt (**7**). The mixture of 6 (1.24 g, 3.46 mmol), 5-iodopyrimidin-2-amine (1.15 g, 5.18 mmol), $Pd(PCy3)_2Cl_2$ (170 mg, 0.24 mmol), cesium carbonate (4.51 g, 13.8 mmol) and DMSO (16.5 ml, 232 mmol) was stirred at 120°C for 3 h under N_2. The mixture was diluted with water and brine, and extracted with EtOAc. The organic layer was collected, washed with brine, dried over $MgSO_4$, and concentrated *in vacuo*. The residue was purified by silica gel column chromatography (n-hexane-ethyl acetate = 100 : 0-80 : 20) to yield crude product. The crude product was subjected to amino silica gel column chromatography and eluted with (ethyl acetate-methanol = 100 : 0-50 : 50) to remove byproducts. The amino silica gel, including the desired product, was subjected to water/EtOAc/AcOH (100 mL-100 mL-18 mL). The mixture was stirred at room temperature for 10 min, the insoluble materials were filtered off, and further elution with EtOAc-AcOH (30 mL-6 mL) was carried out 4 times. From the combined filtrate, the organic layer was collected, washed with water and brine, dried over $MgSO_4$, and concentrated in vacuo. The residue was dissolved with EtOAc/THF/saturated $NaHCO_3$aq. (120 ml-30 ml-30 ml). The organic layer was collected, washed with saturated $NaHCO_3$aq, brine, dried over $MgSO_4$, and concentrated in vacuo. This solid was triturated with EtOAc, and the precipitate was collected by filtration to yield crude product as a white solid (872 mg). The obtained solid was purified by silica gel column chromatography (n-hexane-ethyl acetate = 100 : 0-0 : 100), and triturated with EtOAc. The precipitate was collected by filtration to yield free form of the desired product (635 mg). Additional batches with 4.05 times scale and 4.12 times scale were carried out in a

similar manner to obtain free form of the desired product (4.83 g). All obtained free form of the desired product were combined, and dissolved with AcOH (24.8 mL) and DMSO (66 mL) at 50°C. The solution was filtered to remove small insoluble materials with washing with AcOH (24.8 mL). Water (50 mL) was added dropwise to the filtrate at 50°C. The mixture was allowed to cool to 25°C for 30 min. The precipitate was collected by filtration, washed with EtOH-water (1/10, 33 mL) 3 times and dried under vacuum at 50°C to yield 7 (5.53 g, 20% for 2 steps) as a white solid. 1H NMR (300 MHz, DMSO-d6) δ 1.91 (3H, s), 3.94 (3H, s), 7.14-7.37 (4H, m), 8.07 (1H, d, J = 2.6 Hz), 8.43 (2H, s), 8.52 (1H, d, J = 2.6 Hz), 10.46 (1H, s), 11.94 (1H, s). Anal. Calcd for C20H16ClF2N5O5S: C, 46.93; H, 3.15; N, 13.68. Found: C, 46.85; H, 3.17; N, 13.64.

GCN2 kinase assay

Recombinant GCN2 (1 nmol/L) protein (Carna Biosciences) was pre-incubated with GCN2 inhibitors for 60 min and then incubated with ATP (K_M value of GCN2 = 190 μmol/L) and the green fluorescent protein-eIF2α substrate (130 nmol/L) at 25°C. The amount of phosphorylated substrate was determined using the LanthaScreen Tb-anti-p-eIF2α (pSer52) antibody kit (Thermo Fisher Scientific). The IC_{50} value of eIF2α kinase was measured using the XLfit software (IDBS).

Kinase panel

Kinase selectivity of GCN2iA was evaluated at 1 μmol/L using a panel of 27 kinases that covers major kinase families. Serine/threonine kinase assays were performed using [γ-33P] ATP in 96-well plates. The reaction conditions were optimized for each kinase: p38α (100 ng/well enzyme, 1 μg/well myelin basic protein [MBP], 0.1 μCi/well [γ-33P] ATP, 60-min reaction at 30°C); extracellular signal-regulated protein kinase 1 (ERK1; 100 ng/well enzyme, 2 μg/well MBP, 0.1 μCi/well [γ-33P] ATP, 60-min reaction at 30°C); protein kinase C ζ (PKCζ; 25 ng/well enzyme, 2 μg/well MBP, 0.1 μCi/well [γ-33P] ATP, lipid activator [Millipore], 60-min reaction at 30°C]; c-Jun N-terminal kinase 1 (JNK; 10 ng/well enzyme, 1 μg/well c-Jun, 0.1 μCi/well [γ-33P] ATP, 60-min reaction at 30°C); mitogen-activated protein kinase 1 (MEK1; 100 ng/well enzyme, 0.3 μg/well glutathione *S*-transferase-ERK1 [K71A], 0.2 μCi/well [γ-33P] ATP, 20-min reaction at 25 °C); Aurora-B (50 ng/well enzyme, 30 μmol/L Aurora-substrate peptide, 0.2 μCi/well [γ-33P] ATP, 60-min reaction at 25°C); protein kinase A (PKA; 3 nmol/L enzyme, 1 μmol/L PKA-substrate peptide [Millipore], 0.2 μCi/well [γ-33P] ATP, 10-min reaction at 25°C); cyclin-dependent kinase 2 in complex with cyclin A (CDK2/CycA; 1.8 mU/well enzyme, 1 μg/well histone H1, 0.2 μCi/well [γ-33P]ATP, 20-min reaction at 25°C); casein kinase 1 δ (CK1δ; 120 ng/well enzyme, 2.4 μmol/L CK1tide [Millipore], 0.2 μCi/well [γ-33P] ATP, 20-min reaction at 25°C); checkpoint kinase 1 (CHK1; 30 ng/well enzyme, 25 μM CHKtide [Millipore], 0.2 μCi/well [γ-33P] ATP, 10-min reaction at 25°C); GSK-3β (25 ng/well enzyme, 0.2 μg/well GSK3-substrate peptide [Millipore], 0.1 μCi/well [γ-33P] ATP, 30-min reaction at 25°C); Akt1 (120 ng/well enzyme, 5 μmol/L Akt1-substrate [Millipore], 0.2 μCi/well [γ-33P] ATP, 20-min reaction at 25°C); apoptosis signal-regulating kinase 1 (ASK1; 25 ng/well enzyme, 2 μg/well MBP, 0.1 μCi/well [γ-33P] ATP, 60-min reaction at 25°C); mitogen-activated protein kinase-activated protein kinase 2 (MAPKAP2; 300 ng/well enzyme, 0.5 μmol/L KKLNRTLSVA-NH2, 0.1 μCi/well [γ-33P] ATP, 10-min reaction at 25°C);

rho-associated, coiled-coil-containing protein kinase 1 (ROCK1; 164 ng/well enzyme, 0.5 μmol/L long S6 peptide [Millipore], 0.2 μCi/well [γ-33P] ATP, 10-min reaction at 25°C); polo-like kinase 1 (PLK1; 25 ng/well enzyme, 3 μg/well of casein [Sigma-Aldrich], 0.2 μCi/well [γ-33P] ATP, 60-min reaction at 25°C); interleukin-1 receptor-associated kinase 4 (IRAK4; 27.7 ng/well enzyme, 0.5 μmol/L MBP, 0.2 μCi/well of [γ-33P] ATP, 60-min reaction at 25°C); and cell division cycle 7/activator of S-phase kinase (CDC7/Dbf4 complex; 3.1 ng/well enzyme, 500 ng/well His-tagged minichromosome maintenance complex component 2, 0.2 μCi/well [γ-33P] ATP, 60-min reaction at 25°C). Enzyme reactions were performed in 25 mmol/L HEPES (pH 7.5) supplemented with 10 mmol/L magnesium acetate, 1 mmol/L dithiothreitol, and 500 nmol/l ATP, and containing an optimized concentration of enzyme, substrate, and radiolabeled ATP, as described above, in a total volume of 50 μL. Prior to initiating the kinase reaction, the compound and enzyme were incubated for 5 min at the reaction temperature described; the reaction was then initiated by adding ATP. After the reaction periods mentioned, the reactions were terminated by adding 10% trichloroacetic acid. The [γ-33P]-phosphorylated proteins were filtered into 96-well filter plates using a cell harvester (PerkinElmer), and free [γ-33P] ATP was removed by washing with 3% phosphoric acid. The plates were dried, and 40 μL MicroScint0 (PerkinElmer) was added. Radioactivity was measured using a TopCount scintillation counter (PerkinElmer).

Assays for tyrosine kinases were performed using the Alphascreen system (PerkinElmer) in 384-well plates at 25°C. The reaction conditions for these kinase assays were optimized for each kinase: VEGF receptor 2 (VEGFR2; 19 ng/mL enzyme, 10 μM ATP, 10-min reaction, PY-100-conjugated acceptor beads [PY-100]); proto-oncogene tyrosine-protein kinase (SRC; 0.33 ng/mL enzyme, 2 μmol/L ATP, 10-min reaction, PY-100); IRK (100 ng/mL enzyme, 10 μmol/L ATP, 60-min reaction, PT66); focal adhesion kinase (FAK; 30 ng/mL enzyme, 2 μmol/L ATP, 20-min reaction, PT66); ephrin receptor A5 (EphA5; 1 ng/mL enzyme, 2 μmol/L ATP, 10-min reaction, PY-100); Janus kinase 1 (JAK1; 100 ng/mL enzyme, 0.2 μmol/L ATP, 10-min reaction, PT66); and endothelial growth factor receptor (EGFR; 100 ng/mL enzyme, 1.0 μmol/L ATP, 10-min reaction, PT66). The enzyme reactions were performed in 50 mmol/L Tris-HCl (pH 7.5) with 5 mmol/L $MnCl_2$, 5 mmol/L $MgCl_2$, 0.01% Tween-20, 2 mmol/L dithiothreitol, 0.1 μg/mL biotinylated poly-GluTyr (4 : 1), and optimized concentrations of enzyme and ATP, as described. Prior to the initiation of the kinase reaction, the compound and enzyme were incubated for 5 min at 25°C. The reaction was then initiated by adding ATP. The reactions were stopped by the addition of 25 μL of 100 mmol/L EDTA, 10 μg/mL Alphascreen streptavidin donor beads (PerkinElmer), and 10 μg/mL acceptor beads in 62.5 mmol/L HEPES (pH 7.4), 250 mmol/L NaCl, and 0.1% bovine serum albumin. The plates were incubated in the dark for > 12 h, followed by analysis using an EnVision plate reader (PerkinElmer).

Assays for phosphatidylinositol-4,5-bisphosphate 3-kinase α (PI3Kα) were performed using a phospholipid FlashPlate coated with 5 μmol/L L-α-phosphatidyl-D-myo-inositol 4,5-diphosphate. The reaction conditions were optimized for PI3Kα (80 ng/well enzyme, 0.15 μCi/well of [γ-33P] ATP, 60-min reaction at 25°C), and radioactivity was measured using a TopCount scintillation counter (PerkinElmer).

For kinome-wide profiling, kinase selectivity of GCN2iB was evaluated at 1 μmol/L using a panel of 468 kinases at DiscoveRx (KINOMEscan). The platform employs an active site-directed competition

binding assay to quantitatively measure interactions between test compounds and kinases.

Short interfering RNA

ASNS or ATF4 siRNAs were purchased from GE Dharmacon (OnTARGETplus) or Thermo Fisher Scientific (Silencer Select), respectively. Human Cell Death siRNA was purchased from Qiagen and used as a positive control for transfection efficiency. The sequences of the sense siRNAs are shown below:
ASNS-1: 5′-GGG UAG AGA UAC AUA UGG A-3′; ASNS-2: 5′-UAU GUU GGA UGG UGU GUU U-3′; ASNS-3: 5′-GGU GAA AUC UAC AAC CAU A-3′; ATF4-1: 5′-GCC UAG GUC UCU UAG AUG A-3′; ATF4-2: 5′-CCC UGU UGG GUA UAG AUG A-3′; and ATF4-3: 5′-GUG AGA AAC UGG AUA AGA A-3′.

Transfection and western blot analysis

Adherent or floating cells were transfected with siRNAs using Lipofectamine RNAi MAX (Invitrogen) or GenomeONE with inactivated Sendai virus envelope (Ishihara Sangyo), respectively. Western blot analysis was performed as described in a previous study (Ref; 2).

The following antibodies were used for the western blot analysis: anti-phospho-Ser473-Akt (#4060, 1:1000), -ATF4 (#11815, 1:1000), -cleaved PARP (#5625, 1:1000), -eIF2α (#5324, 1:2000), -phospho-Ser51-eIF2α (#3597, 1:1000), -phospho-Thr202/Tyr204-ERK (#4370, 1:1000), -GCN2 (#3302, 1:1000), -phospho-Thr183/Tyr185-JNK (#9251, 1:1000), -phospho-Thr180/Tyr182-p38 (#9211, 1:1000), -PERK (#3192, 1:1000), -Sestrin2 (#8487, 1:1000), -S6K (#9202, 1:1000), and -phospho-Thr389-S6K (#9234, 1:1000) (Cell Signaling Technology); anti-ASNS (#14681-1-AP, 1:2000) and -GADD34 (#10449-1-AP, 1:1000) (Proteintech); anti-HSP90 (#610419, 1:2000, BD Transduction Laboratories); anti-phospho-Thr899-GCN2 (#ab75836, 1:1000, Abcam); and anti-puromycin (#MABE343, 1:1000, Millipore). eIF2α and HSP90 were used as loading controls.

Amino acid measurement

Cells, culture medium, tissue, and plasma ($N = 3$) were homogenized in ice-cold methanol using a ShakeMaster Auto (BioMedical Science) and centrifuged at 15,000 × *g* for 5 min. The supernatant was dried by nitrogen stream and derivatized using N-methyl-N-(tert-butyldimethylsilyl) trifluoroacetamide. The reaction mixture was injected into an Agilent 7890A series GC system in the split injection mode (10/1 [v/v]) using a GC injector 80 autosampler (Agilent Technologies). GC separation was performed using an Agilent J&W GC column HP-5 ms (30 m × 0.25 mm i.d., df = 0.25 μm) and a temperature gradient (100°C for 4 min, from 100°C to 285°C at 4 °C/min, from 285°C to 325°C at 4 °C/min, and 325°C for 2 min) with a constant flow of helium gas at 1 mL/min. The eluate was ionized by electron-impact ionization (70 eV) at an ion-source temperature of 230°C and introduced into an Agilent 7010B triple-quadrupole mass spectrometer (Agilent Technologies). Each target molecule was detected by selected ion monitoring, the parameters for which were optimized using standard reagents.

For quantitation of amino acids, a standard solution was prepared by mixing all amino acids at concentrations of 0.2, 1, 2, 10, 20, 100, and 200 nmol/L. Internal standard solution 1 (IS1) was prepared by

diluting with (U-13C3, U-15N)-cell-free amino acid mix (20 AA; Cambridge Isotope Laboratories) until the total amino acid concentration reached 2 mg/mL. Internal standard solution 2 (IS2) was diluted with (U-13C3, U-15N)-cysteine (5 μmol/L). Each standard solution (25 μL) was mixed with 50 μL of methanol, which was used as the blank control, and 10 μL of IS1 or IS2. The mixture was dried, derivatized, and analyzed using GC-MS. Quantitative reliability was confirmed by the linearity of the calibration curve (R^2 > 0.99) and the accuracy (< 20%) and precision (< 20%; N = 6) of the spike-and-recovery test.

Gene expression data for cancer cell lines

Data were collected from public databases associated with the Cancer Cell Line Encyclopedia and GlaxoSmithKline. All data were obtained as CEL files and signal values were extracted using the MAS5.0 algorithm.

Microarray analysis

Total RNA was extracted using the RNeasy Miniprep kit (Qiagen), according to the manufacturer's protocol. Preparation of cRNA, hybridization, and microarray scanning were performed using Macrogen, according to the manufacturer's protocol (Agilent Technologies). Labeled cRNA was hybridized to Agilent SurePrint G3 human GE 8X60K microarrays (Agilent Technologies), which were immediately scanned using an Agilent microarray scanner D (Agilent Technologies). The results of the microarray were obtained using Agilent Feature Extraction software (v.11.0; Agilent Technologies). Pathway and upstream analyses were performed using Ingenuity Pathway Analysis (Qiagen).

Cell viability assay

Cell viability was assessed using the CellTiter-Glo luminescent cell viability assay (Promega), according to the manufacturer's protocol. Sigmoidal dose-response (variable slope) curves were fitted using a nonlinear regression analysis. The IC_{50} or IC_{70} values of the chemical compounds or enzymes were calculated using GraphPad Prism software v.6.

Caspase 3/7 assay

Caspase 3/7 activity was assessed using the Caspase-Glo 3/7 assay (Promega), according to the manufacturer's protocol.

Animal study

A suspension of CCRF-CEM, HPB-ALL, MV-4-11, or SU.86.86 cells (1×10^7 cells/site) was subcutaneously injected into the right flanks of 6-week-old female SCID mice (C.B17/Icr-scid/scid Jcl; CLEA). Tumor volume was calculated as volume = $L \times l^2 \times 1/2$, where L represents the longest diameter across the tumor and l represents the corresponding perpendicular distance. Body weight was also measured. To assess the anti-tumor activity, mice with tumor mass ~200 mm^3 were sorted into treatment groups (N = 5/group) (to ensure similarity in mean tumor volume among the groups). The tumors were monitored and mice were

euthanized when an endpoint (defined as tumor volume > 2,000 mm^3, severe ataxia, and body weight loss > 20% compared with the body weight on the day of randomization) was reached, or at the end of the study, whichever came first. From the next day of randomization, GCN2 inhibitors or ASNase dissolved in distilled water containing 0.5% methylcellulose or 5% glucose was orally or intraperitoneally administered to mice bearing the xenografts for 7 to 10 days, respectively. T/C (%), an index of anti-tumor activity, was calculated by comparing the mean change in tumor volume during the treatment period in the control and treated groups. For western blot analysis, tumors were homogenized with Lysing Matrix I (MP Biomedicals) in a lysis buffer (10% glycerol, 1% sodium dodecyl sulfate, and 62.5 mmol/L Tris-HCl [pH 7.5] with protease and phosphatase inhibitors, cOmplete Mini and PhosSTOP, respectively; Sigma-Aldrich).

For the disseminated leukemia model, suspension of MOLT-3 cells (1×10^7 cells/head) was inoculated in to SCID mice via the tail vein. Fourteen days after inoculation, mice were assigned into treatment groups (N = 7/group) randomly based on body weight. From the next day of randomization, the compounds were administered to mice for 28 days. The survival rate was determined by the Kaplan-Meier analysis.

The mice were housed and maintained in accordance with the institutional guidelines established by the Institutional Animal Care and Use Committee, in a facility accredited by the American Association for Accreditation of Laboratory Animal Care. All animal experimental protocols were approved by the Institutional Animal Care and Use Committee.

Statistical analysis

To assess the *in vitro* anti-proliferative effects of the GCN2 inhibitors in the presence or absence of ASNase for the cell-panel study, a paired *t*-test comparison was performed using the GraphPad Prism software (v.6; GraphPad Software). To assess the correlation between variables, linear regression analysis was performed, and the correlation coefficient was determined by Pearson's correlation using the GraphPad Prism software. To assess the *in vivo* antitumor effect of the treatment methods, Dunnett's multiple-comparison test was performed, followed by one-way ANOVA with T/C (%) values. A two-way ANOVA was performed to examine the primary effects of treatment with the GCN2 inhibitor or the ASNase, as well as the combinatorial effect of treatments with T/C values. The combinatorial effect was assessed using the following criteria: 1) synergistic effect, defined as the significant differences observed in the combined effect of treatment with a GCN2 inhibitor and ASNase, along with the enhancements in effect caused by each treatment; 2) additive effect, defined as significant differences observed in the primary effect of treatment with a GCN2 inhibitor or ASNase, but not in their combined form; and 3) antagonistic effect, defined as the significant differences observed in the combined effect of treatment with a GCN2 inhibitor and ASNase, along with the reductions in effect caused by each treatment. To assess the effect of treatment on survival curve in the disseminated model, log-rank test was performed between vehicle-treated group and treatment groups. Cox regression analysis was performed to examine the main effect of a GCN2 inhibitor and ASNase, and effect of interaction between the 2 treatments with survival curves using SAS version 9.1.3 (SAS Institute Inc.). Other statistical analyses for in vivo studies were conducted using EXSUS (Release 8.0; CAC

Croit Corporation). The different groups were compared using Bonferroni's multiple-comparison test, unless otherwise mentioned. Differences were considered significant when $P < 0.05$.

Cell lines and culture

Cell lines were cultured at 37°C with 5% CO_2 in the recommended medium supplemented with 10%–20% FBS. The cell lines for which the asparagine-free medium (e.g., Dulbecco's modified Eagle's medium) was recommended were maintained in RPMI1640 medium. We established two ASNase-resistant cell lines (MOLT-4-R1 and-R2; two replicates) by treating them with increasing concentrations of ASNase (0.00001–1 U/mL) for 4 months. All cell lines were stocked after *Mycoplasma* testing (at the Central Institute for Experimental Animals) and used within 2 months of resuscitation. The authors did not perform any authentication. Detailed information on the cell lines is provided as follows.

Cell line	Cell type	Source	Year
CMK-11-5	Acute myelogenous leukemia	JCRB	2014
EOL-1	Acute myelogenous leukemia	DSMZ	2014
GF-D8	Acute myelogenous leukemia	DSMZ	2014
HEL.92.1.7	Acute myelogenous leukemia	ATCC	2014
HL-60	Acute myelogenous leukemia	ATCC	2014
HNT-34	Acute myelogenous leukemia	RIKEN	2015
Kasumi-1	Acute myelogenous leukemia	JCRB	2014
KG-1	Acute myelogenous leukemia	ATCC	2014
KG-1a	Acute myelogenous leukemia	RIKEN	2015
KO52	Acute myelogenous leukemia	JCRB	2014
M-07e	Acute myelogenous leukemia	DSMZ	2014
MKPL-1	Acute myelogenous leukemia	JCRB	2014
ML-1	Acute myelogenous leukemia	ECACC	2015
ML-2	Acute myelogenous leukemia	DSMZ	2014
MOLM-16	Acute myelogenous leukemia	DSMZ	2014
MV-4-11	Acute myelogenous leukemia	ATCC	2016
NKM-1	Acute myelogenous leukemia	JCRB	2014
NOMO-1	Acute myelogenous leukemia	JCRB	2014
OCI-AML3	Acute myelogenous leukemia	DSMZ	2014
OCI-M2	Acute myelogenous leukemia	DSMZ	2014
PL-21	Acute myelogenous leukemia	JCRB	2014
SKM-1	Acute myelogenous leukemia	JCRB	2014
SKNO-1	Acute myelogenous leukemia	JCRB	2015
TF-1	Acute myelogenous leukemia	ATCC	2014

TF-1a	Acute myelogenous leukemia	ATCC	2014
THP-1	Acute myelogenous leukemia	ATCC	2014
BALL-1	Acute lymphoblastic leukemia	JCRB	2015
CCRF-CEM	Acute lymphoblastic leukemia	ATCC	2014
CCRF-HSB-2	Acute lymphoblastic leukemia	JCRB	2015
CCRF-SB	Acute lymphoblastic leukemia	JCRB	2015
DND-41	Acute lymphoblastic leukemia	DSMZ	2014
HAL-01	Acute lymphoblastic leukemia	RIKEN	2014
HPB-ALL	Acute lymphoblastic leukemia	DSMZ	2014
Jurkat	Acute lymphoblastic leukemia	RIKEN	2014
Loucy	Acute lymphoblastic leukemia	ATCC	2015
MOLT-3	Acute lymphoblastic leukemia	ATCC	2014
MOLT-4	Acute lymphoblastic leukemia	ATCC	2014
NALM-6	Acute lymphoblastic leukemia	RIKEN	2014
PALL-2	Acute lymphoblastic leukemia	JCRB	2015
Peer	Acute lymphoblastic leukemia	JCRB	2015
Reh	Acute lymphoblastic leukemia	ATCC	2014
RS4;11	Acute lymphoblastic leukemia	ATCC	2015
SUP-B15	Acute lymphoblastic leukemia	ATCC	2015
TALL-1	Acute lymphoblastic leukemia	DSMZ	2014
Tanoue	Acute lymphoblastic leukemia	RIKEN	2015
TMD5	Acute lymphoblastic leukemia	JCRB	2015
AsPC-1	Pancreatic cancer	ATCC	2011
BxPC-3	Pancreatic cancer	ATCC	2013
Capan-1	Pancreatic cancer	ATCC	2011
Capan-2	Pancreatic cancer	ATCC	2011
CFPAC-1	Pancreatic cancer	ATCC	2011
DAN-G	Pancreatic cancer	DSMZ	2011
HPAC	Pancreatic cancer	ATCC	2011
HPAF-II	Pancreatic cancer	ATCC	2014
HuP-T3	Pancreatic cancer	ECACC	2011
HuP-T4	Pancreatic cancer	ECACC	2016
KP-4	Pancreatic cancer	JCRB	2011
Panc 02.03	Pancreatic cancer	ATCC	2011
Panc 04.03	Pancreatic cancer	ATCC	2011
Panc 05.04	Pancreatic cancer	ATCC	2011
PK-45H	Pancreatic cancer	RIKEN	2011

PK-59	Pancreatic cancer	RIKEN	2011
PL45	Pancreatic cancer	ATCC	2011
SU.86.86	Pancreatic cancer	ATCC	2011
SUIT2	Pancreatic cancer	JCRB	2011
TCC-PAN2	Pancreatic cancer	JCRB	2011
COLO-205	Colorectal cancer	ATCC	2014
HCT-116	Colorectal cancer	ATCC	2013
HCT-15	Colorectal cancer	ATCC	2012
HT-29	Colorectal cancer	ATCC	2013
SW1417	Colorectal cancer	ATCC	2014
SW48	Colorectal cancer	ATCC	2013
SW620	Colorectal cancer	ATCC	2014
SW948	Colorectal cancer	ATCC	2014
T84	Colorectal cancer	ATCC	2013
OCI-LY3	Diffuse large B-cell lymphoma	DSMZ	2015
Pfeiffer	Diffuse large B-cell lymphoma	ATCC	2012
SU-DHL-10	Diffuse large B-cell lymphoma	DSMZ	2012
SU-DHL-2	Diffuse large B-cell lymphoma	ATCC	2015
SU-DHL-4	Diffuse large B-cell lymphoma	DSMZ	2013
Toledo	Diffuse large B-cell lymphoma	ATCC	2012
WSU-DLCL2	Diffuse large B-cell lymphoma	DSMZ	2013
A549	Non-small cell lung cancer	ATCC	2013
NCI-H2228	Non-small cell lung cancer	ATCC	2013
NCI-H23	Non-small cell lung cancer	ATCC	2012
NCI-H460	Non-small cell lung cancer	ATCC	2013
NCI-H522	Non-small cell lung cancer	ATCC	2012
NCI-H661	Non-small cell lung cancer	ATCC	2014
SW1271	Non-small cell lung cancer	ATCC	2014
A2780	Ovarian cancer	ECACC	2014
Caov-3	Ovarian cancer	ATCC	2013
Caov-4	Ovarian cancer	ATCC	2015
OVCAR-3	Ovarian cancer	ATCC	2013
PA-1	Ovarian cancer	ATCC	2014
SKOV-3	Ovarian cancer	ATCC	2013
HepG2	Hepatocellular carcinoma	ATCC	2013
HLE	Hepatocellular carcinoma	JCRB	2016
Huh-7	Hepatocellular carcinoma	JCRB	2015

JHH-4	Hepatocellular carcinoma	JCRB	2016
Li-7	Hepatocellular carcinoma	RIKEN	2014
SK-HEP-1	Hepatocellular carcinoma	ATCC	2014
CAMA-1	Breast cancer	ATCC	2013
MCF7	Breast cancer	ATCC	2014
MDA-MB-361	Breast cancer	ATCC	2013
MDA-MB-468	Breast cancer	ATCC	2014
T47D	Breast cancer	ATCC	2014
SK-MEL-2	Melanoma	ATCC	2014
SK-MEL-24	Melanoma	ATCC	2013
SK-MEL-28	Melanoma	ATCC	2014
SK-MEL-5	Melanoma	ATCC	2014
NCI-H929	Multiple myeloma	ATCC	2012
RPMI-8226	Multiple myeloma	JCRB	2014
U266B1	Multiple myeloma	ATCC	2012
U-2-OS	Osteosarcoma	ATCC	2014

Abbreviations	Full name
ATCC	American Type Culture Collection
DSMZ	Deutsche Sammlung von Mikroorganismen und Zellkulturen
ECACC	The European Collection of Authenticated Cell Cultures
JCRB	Japanese Collection of Research Bioresources
RIKEN	RIKEN

295

Supplementary Figures

A

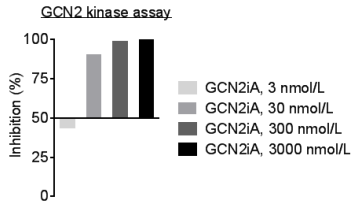

Kinase	IC_{50} (nmol/L)	Inh. (%)	GCN2iA (nmol/L)
GCN2	4.0	44	3
		90	30
		98	300
		100	3,000

B

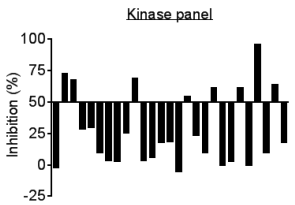

Family	Kinase	Inh. @ 1 μmol/L (%)
TK	EGFR	-2
	VEGFR2	72
	cMET	67
	SRC	29
	FAK	30
	IRK	10
	EphA5	4
	JAK1	5
TKL	IRAK4	26
	TrkA	68
STE	MEK1	-2
	ASK1	-9
CK1	CK1δ	2

Family	Kinase	Inh. @ 1 μmol/L (%)
AGC	PKA	19
	AKT1	-5
	Aurora B	54
	ROCK1	24
	PKCζ	10
CAMK	CHK1	61
	MAPKAP2	0
CMGC	ERK1	3
	CDK2	61
STE	p38α	0
	GSK3β	95
Others	CDC7	10
	PLK1	63
Lipid kinase	PI3Kα	18

Fig. S1. Potency and kinase selectivity of GCN2iA. (*A*) GCN2 kinase assay using GCN2iA. (*B*) Kinase selectivity of GCN2iA in a focused kinase panel.

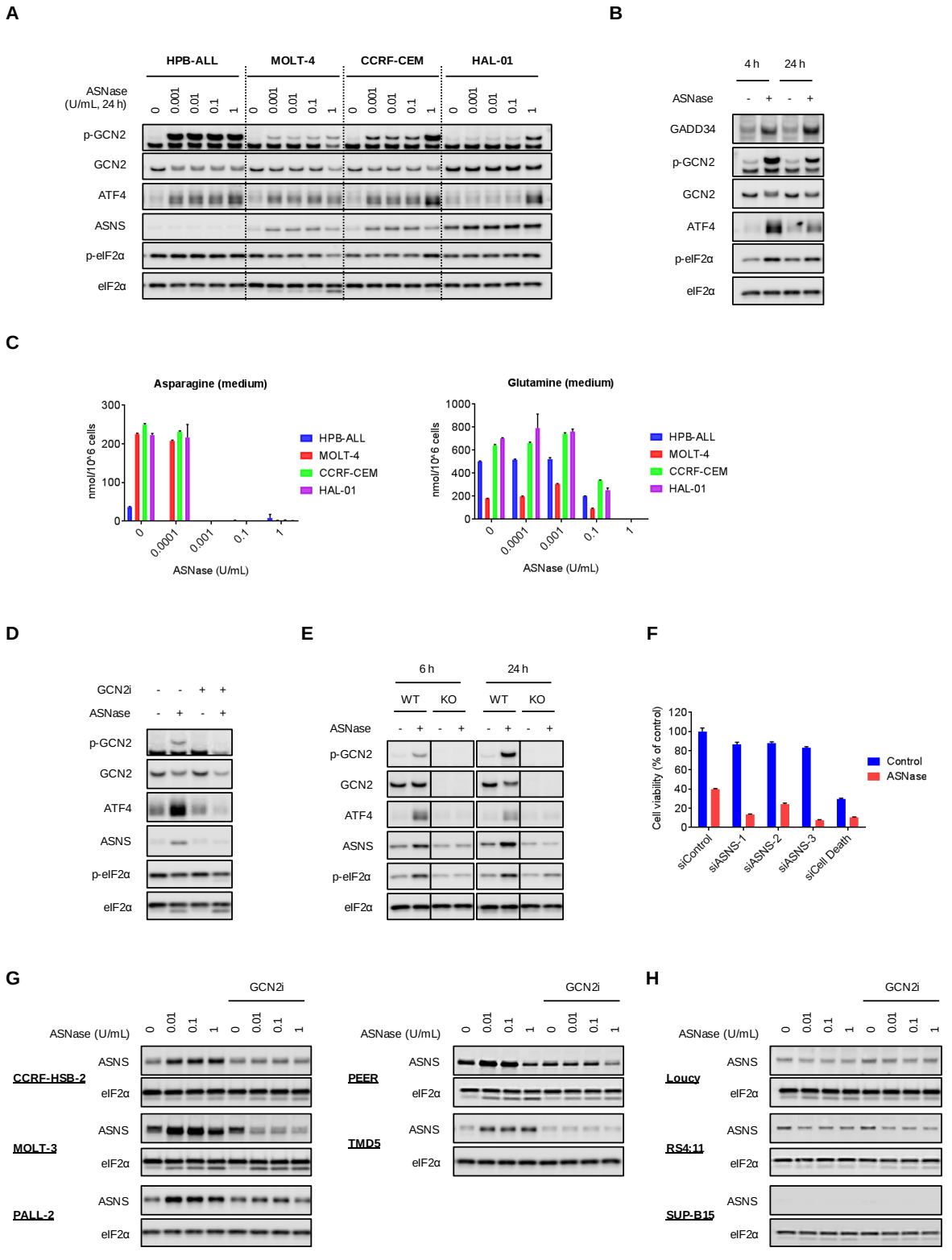

Fig. S2. Characterization of ALL and MEF cells. (*A*) ALL cells were treated with ASNase at the indicated concentrations for 24 h. Cell lysates were analyzed by western blot. (*B*) CCRF-CEM cells were treated with 1 mU/mL ASNase as indicated. Cell lysates were analyzed by western blot. (*C*) ALL cells were treated with

ASNase at the indicated concentrations for 24 h and asparagine or glutamine levels in the culture medium were measured by GC-MS (mean with SD; $N = 3$). (*D*) MOLT-4 cells were treated with 1 mU/mL ASNase and/or 1 μmol/L GCN2iA as indicated for 24 h. Cell lysates were analyzed by western blot. (*E*) MEF cells (GCN2-WT or -KO) were treated with 1 mU/mL ASNase as indicated. Cell lysates were analyzed by western blot. (*F*) CCRF-CEM cells were transfected with siRNA as indicated; 24 h after transfection, cells were treated with 1 mU/mL ASNase for 72 h. Cell viability was measured (mean with SD; $N = 3$). (*G*) ALL cells that were intermediately insensitive to ASNase were treated with ASNase and/or 1 μmol/L GCN2iA as indicated for 24 h. Cell lysates were analyzed by western blot. (*H*) ASNase-hypersensitive ALL cells were treated with ASNase and/or 1 μmol/L GCN2iA as indicated for 24 h. Cell lysates were analyzed by western blot.

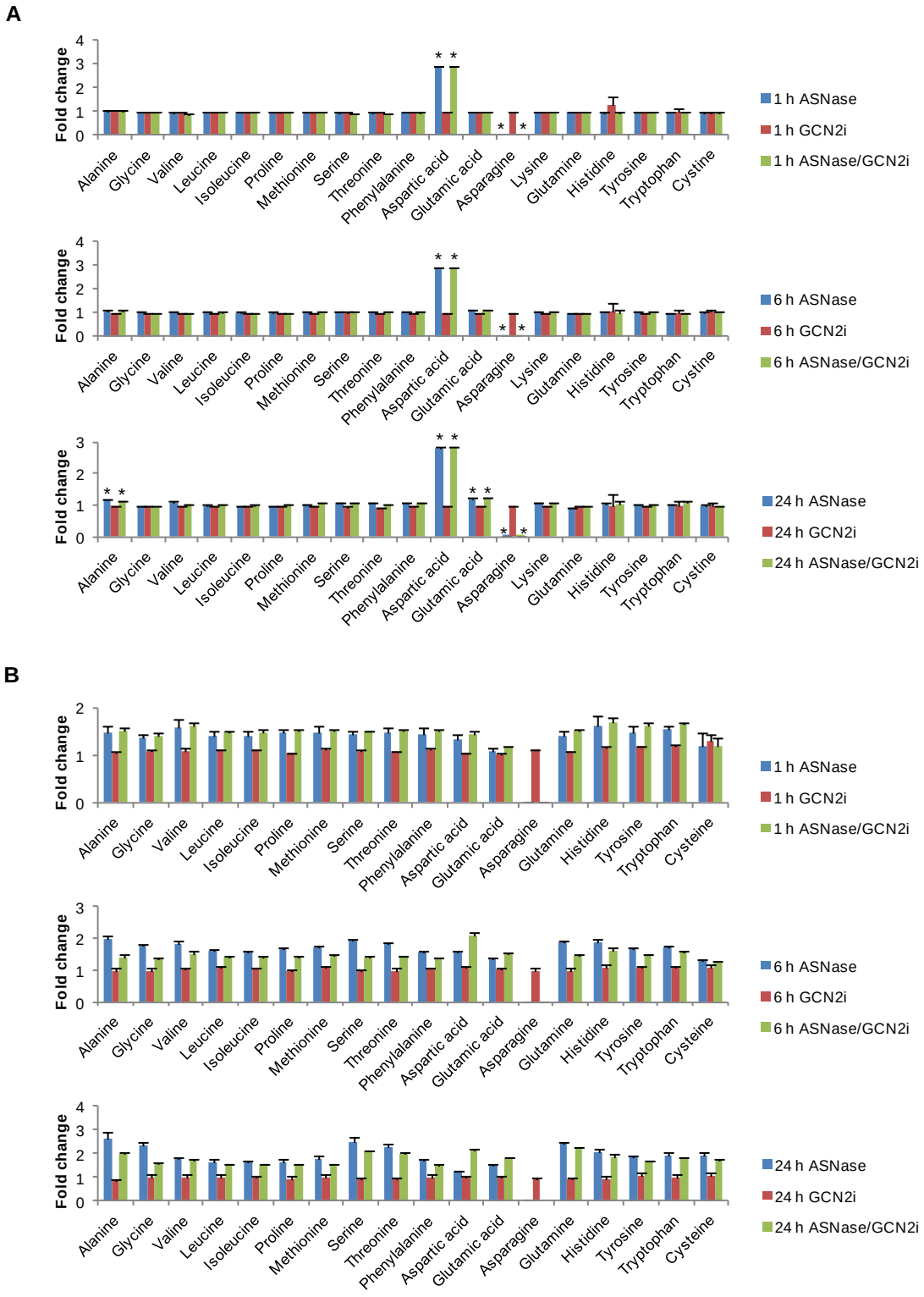

Fig. S3. Effects of GCN2 inhibition on extracellular/intracellular amino acid levels in the presence of ASNase. CCRF-CEM cells were treated with 1 mU/mL ASNase and/or 1 μmol/L GCN2iA as indicated. Amino acid levels in the culture medium (*A*) or in the cells (*B*) were measured by GC-MS (mean with SD; $N = 3$). *$P < 0.01$.

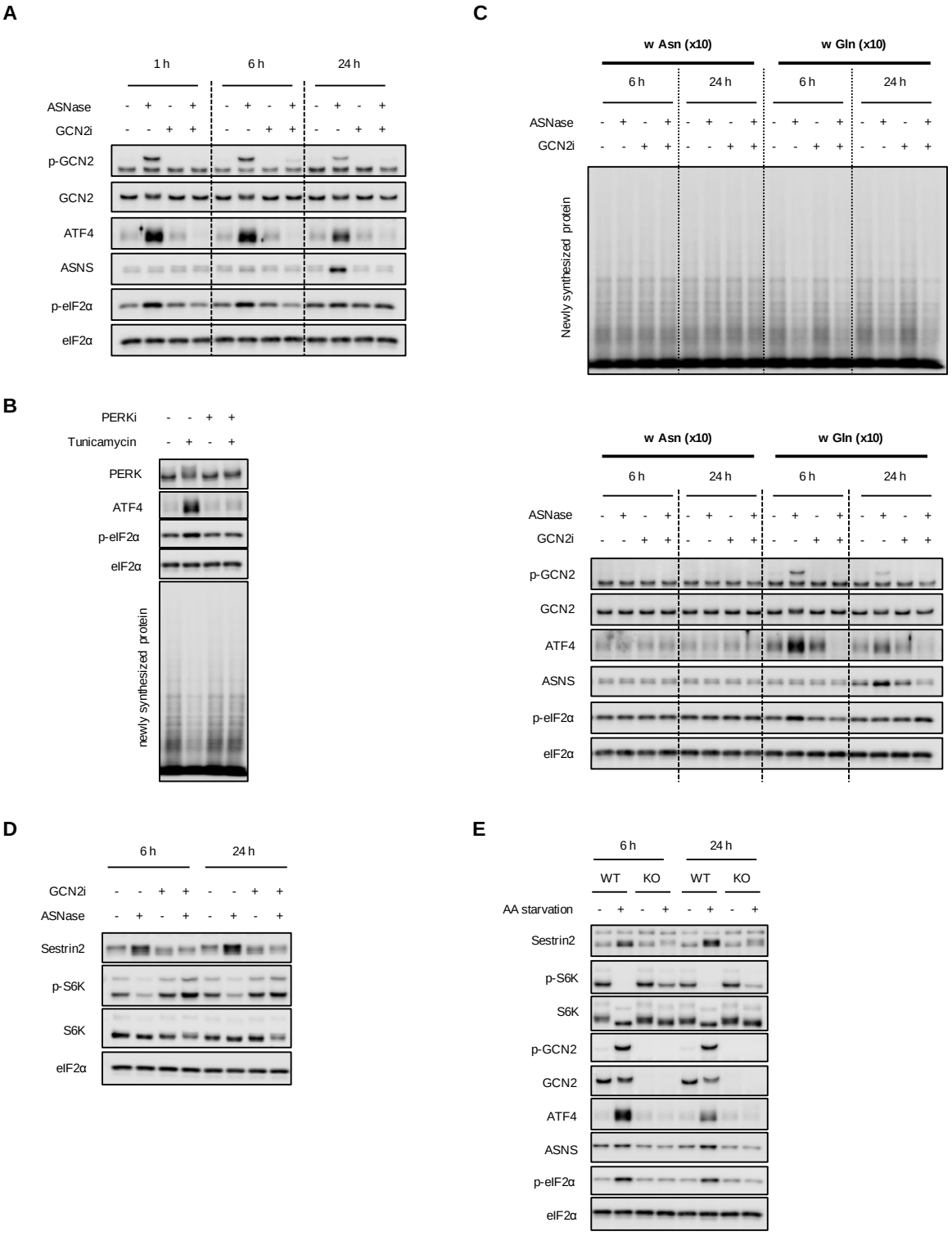

Fig. S4. Suppression of protein translation by GCN2 inhibition in the presence of ASNase. (*A*) CCRF-CEM cells were treated with 1 mU/mL ASNase and/or 1 μmol/L GCN2iA as indicated. Cells were then treated with

10 µmol/L puromycin for 10 min before harvesting. Cell lysates were analyzed by western blot. (*B*) CCRF-CEM cells were treated with 5 µg/mL tunicamycin and/or 1 µmol/L PERK inhibitor as indicated for 1.5 h. Cells were then treated with 10 µmol/L puromycin for 10 min before harvesting. Cell lysates were analyzed by western blot. (*C*) CCRF-CEM cells were treated with 1 mU/mL ASNase and/or 1 µmol/L GCN2iA, along with supraphysiological levels of asparagine (10 ×: 4.3 mmol/L) or glutamine (10 ×: 20 mmol/L) as indicated. Cells were then treated with 10 µmol/L puromycin for 10 min before being harvested. Cell lysates were analyzed by western blot using an anti-puromycin antibody to detect newly synthesized proteins. (*D*) CCRF-CEM cells were treated with 1 mU/mL ASNase and/or 1 µmol/L GCN2iA as indicated. Cell lysates were analyzed by western blot. (*E*) MEF cells (GCN2-WT or -KO) were treated with amino acid-free medium as indicated. Cell lysates were analyzed by western blot.

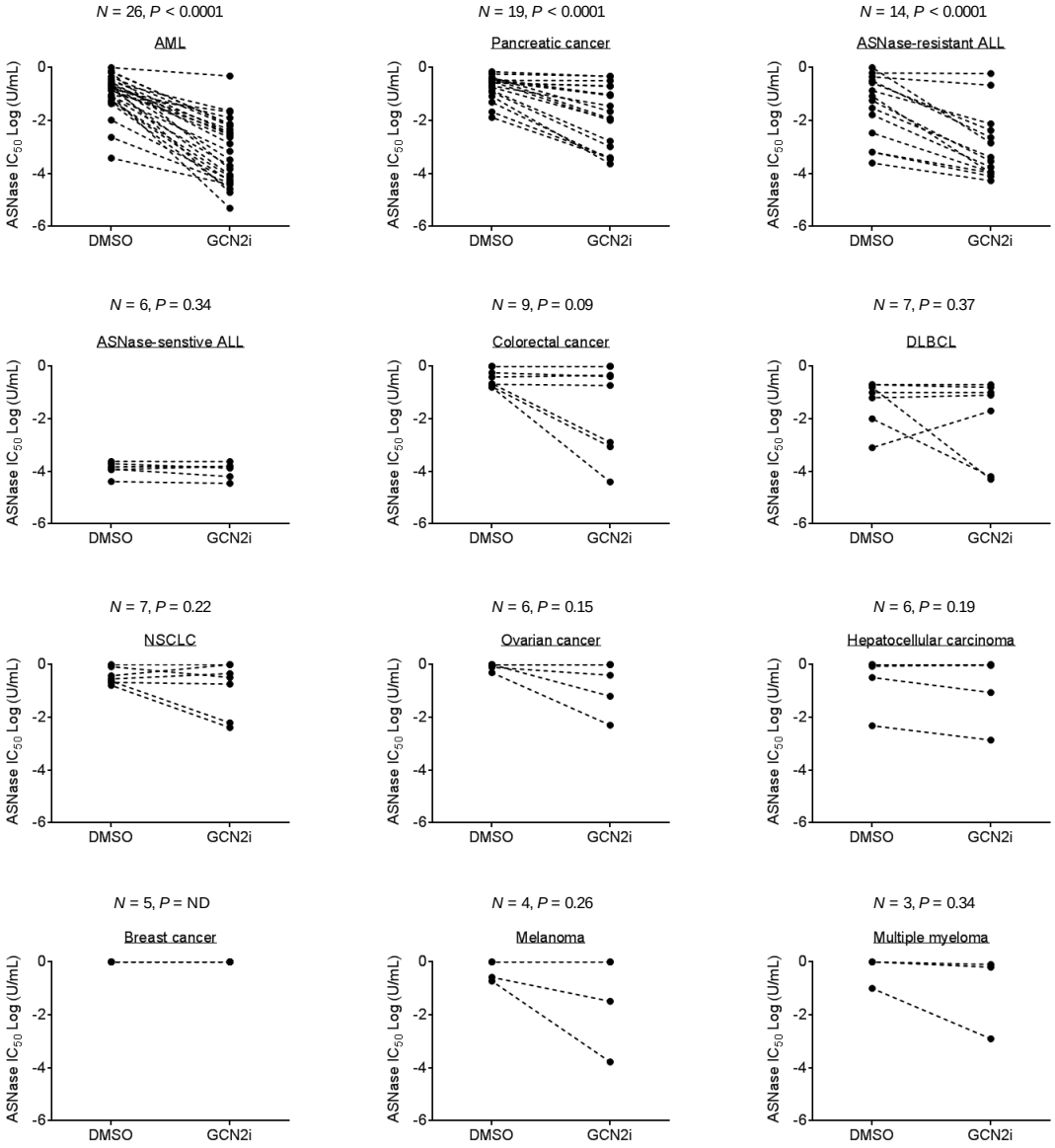

Fig. S5. *In vitro* antiproliferative effects of ASNase-GCN2iA combination treatment in various types of cancer cells. Cell lines of the indicated cancer types were treated with ASNase (0.000001–1 U/mL) and/or 1 μmol/L GCN2iA for 72 h. The cell viability was measured and the mean IC_{50} value of ASNase was calculated (N = 3). Plots for individual cell lines are connected by dotted lines. To assess the combined effects, a paired *t*-test was performed. DLBCL, diffuse large cell B-cell lymphoma; NSCLC, non-small cell lung cancer.

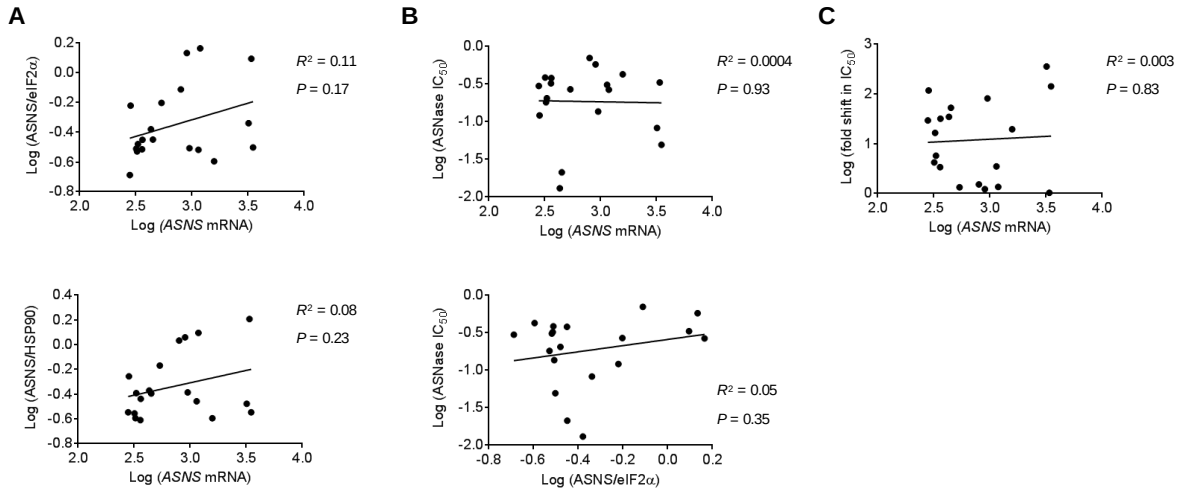

Fig. S6. Correlation between ASNS expression and the combined effects of ASNase treatment with GCN2 inhibition in pancreatic cancer cells. (*A*) Correlation between mRNA and protein levels of ASNS (normalized against eIF2α or HSP90 levels) was analyzed. (*B*) Correlation between IC_{50} value of ASNase and mRNA or protein levels of ASNS (normalized against eIF2α levels) was analyzed. (*C*) Correlation between the combined effects of ASNase treatment with GCN2iA inhibition (fold-change in IC_{50} value) and ASNS mRNA levels (normalized against eIF2α level) was analyzed. Linear regression analysis was performed, and *R*- and *P*-values determined by Pearson's correlation are indicated. PL-45 cells were excluded from the analysis owing to their slow growth during the 72-h culture for the cell viability assay.

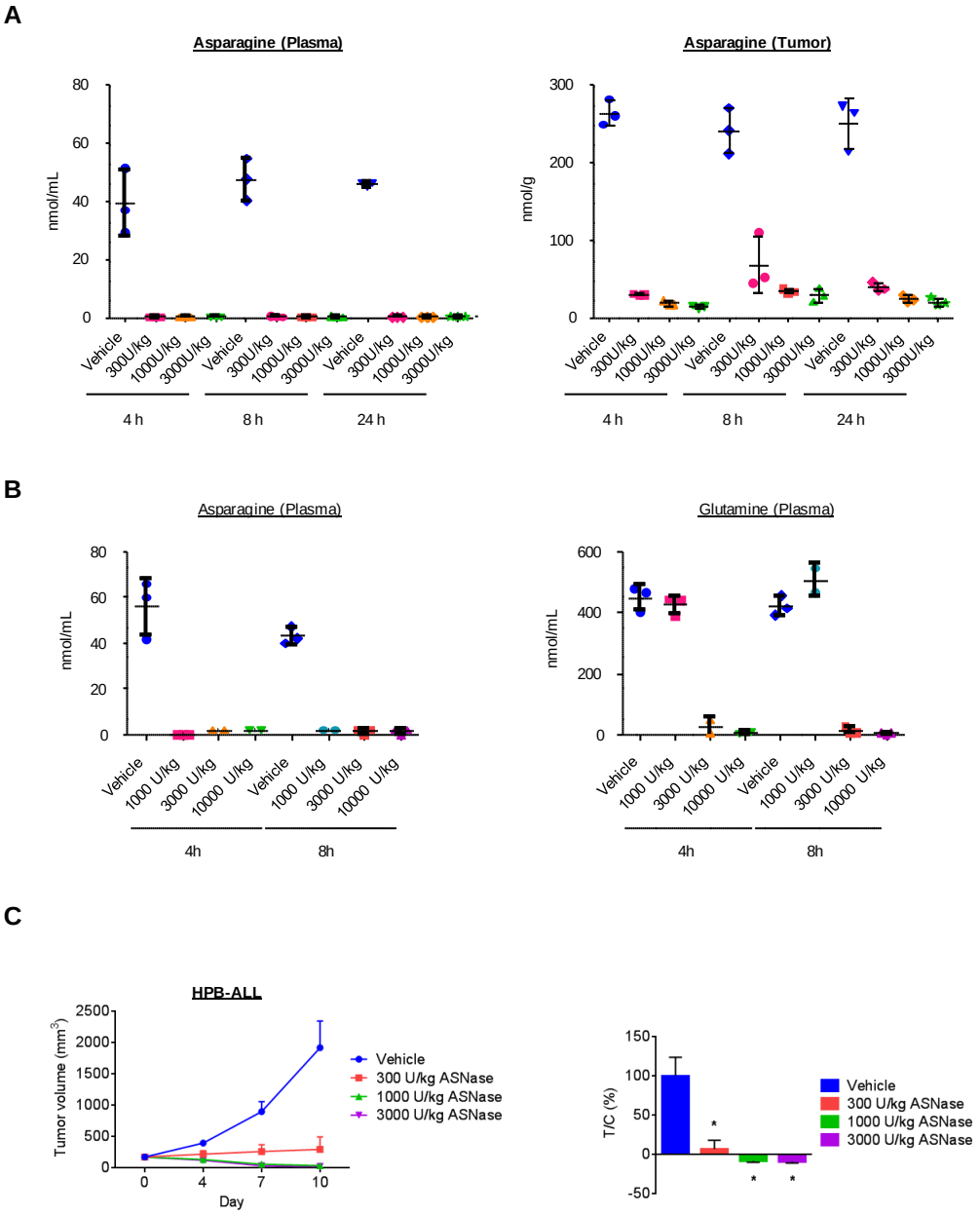

Fig. S7. *In vivo* depletion of asparagine or glutamine in mice by ASNase administration. (*A*) Mice with CCRF-CEM xenografts were treated with ASNase at the indicated doses for 4, 8, or 24 h. Asparagine levels in plasma or tumors were measured by GC-MS. Plots represent values from three biological replicates with SD. (*B*) Mice were treated once daily with ASNase at the indicated doses for 7 days. The asparagine and glutamine levels in plasma were measured with GC-MS 4 or 8 h after the final dose. Plots represent values of two or three biological replicates with SD. (*C*) Mice bearing HPB-ALL xenografts were treated once daily with ASNase at the indicated doses for 10 days. Left, Tumor growth curves; Right, T/C values on day 10. Day 1 indicates the beginning of treatment. Data show mean tumor volume or T/C values with SD ($N = 5$). Dunnett's multiple-comparison test was performed; *$P < 0.0001$ (compared with vehicle-treated control).

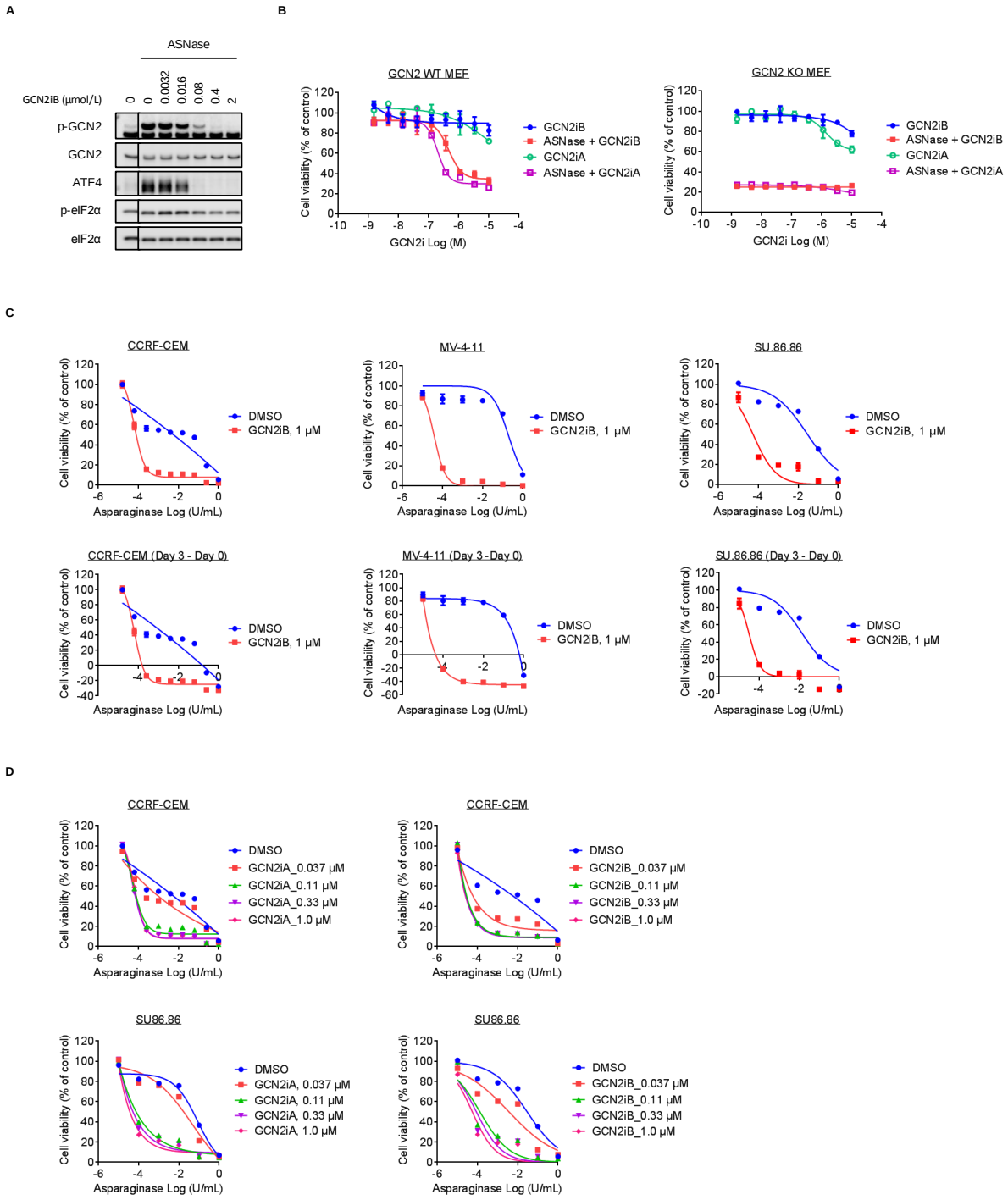

Fig. S8. *In vitro* characterization of GCN2iB. (*A*) CCRF-CEM cells were treated with 1 mU/mL ASNase and/or GCN2iB as indicated for 4 h. Cell lysates were analyzed by western blot. (*B*) MEF cells (GCN2-WT or -KO) were treated with 1 mU/mL ASNase and/or GCN2 inhibitors as indicated for 72 h. Cell viability was measured (mean with SD; $N = 3$). (*C*) CCRF-CEM, MV-4-11, and SU.86.86 cells were treated with ASNase and/or 1 μmol/L GCN2iB as indicated for 72 h. Cell viability was measured at day 0 and day 3 (mean with SD; $N = 3$). (*D*) CCRF-CEM and SU.86.86 cells were treated with ASNase and/or GCN2 inhibitors as indicated for 72 h. Cell viability was measured (mean with SD; $N = 3$).

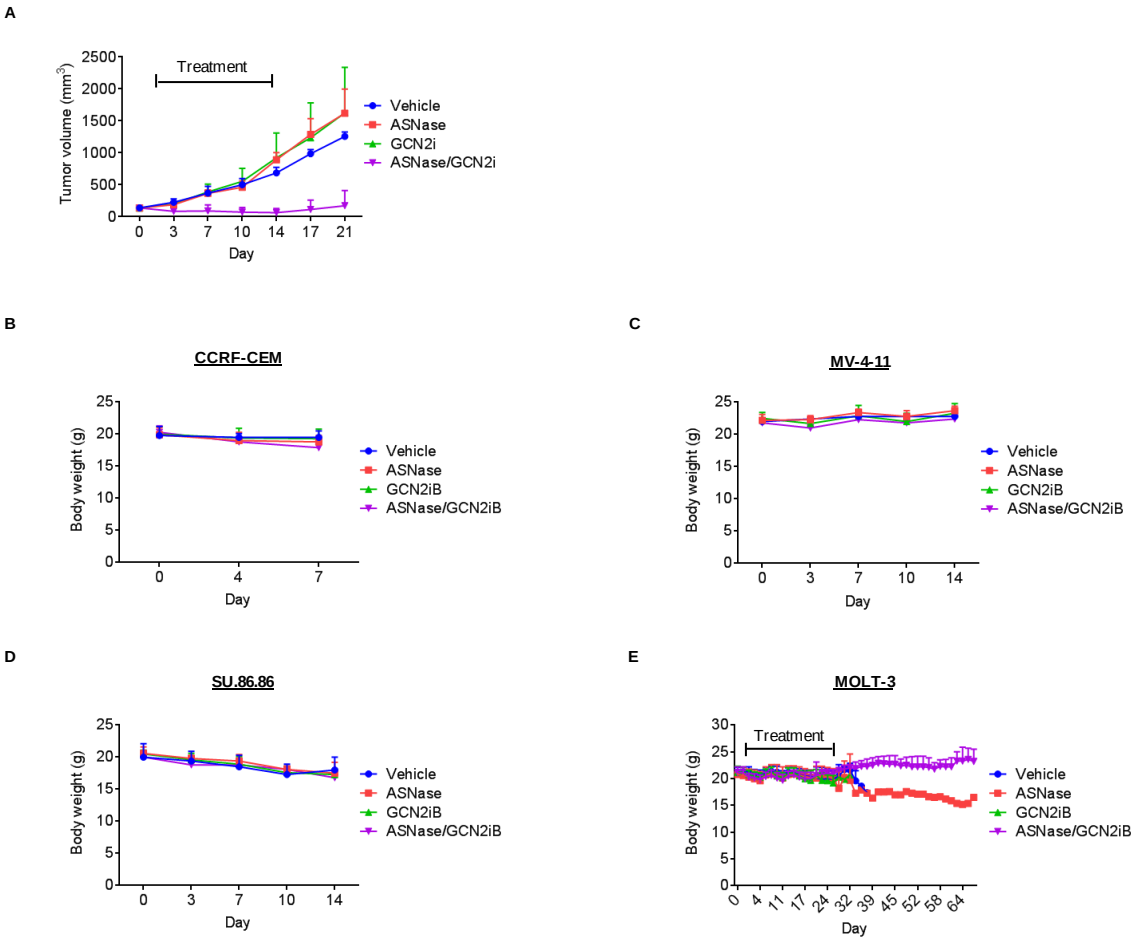

Fig. S9. Changes in the body weight of mice. (*A*) Mice bearing MV-4-11 xenografts were treated first 3 days a week with GCN2iB (10 mpk, twice a day) and/or ASNase (1,000 U/kg, once a day) as indicated for 14 days. Data represent mean tumor volume with SD (N = 5).Tumor volume was measured until 1 week after drug cessation. (*B*) Mice bearing CCRF-CEM xenografts were treated daily with GCN2iB (10 mpk, twice a day) and/or ASNase (1,000 U/kg, once a day) as indicated for 7 days. (*C*) Mice bearing MV-4-11 xenografts were treated first 3 days a week with GCN2iB (10 mpk, twice a day) and/or ASNase (1,000 U/kg, once a day) as indicated for 14 days. (*D*) Mice bearing SU.86.86 xenografts were treated first 3 days a week with GCN2iB (10 mpk, twice a day) and/or ASNase (1,000 U/kg, once a day) as indicated for 14 days. Data represent mean body weight with SD (N = 5). (*E*) MOLT-3 cells were inoculated into SCID mice via the tail vein at 14 days before randomization. From the next day of randomization, mice were treated first 3 days a week with GCN2iB (10 mpk, twice a day) and/or ASNase (1,000 U/kg, once a day) as indicated for 28 days. Data represent mean body weight with SD (N = 7).

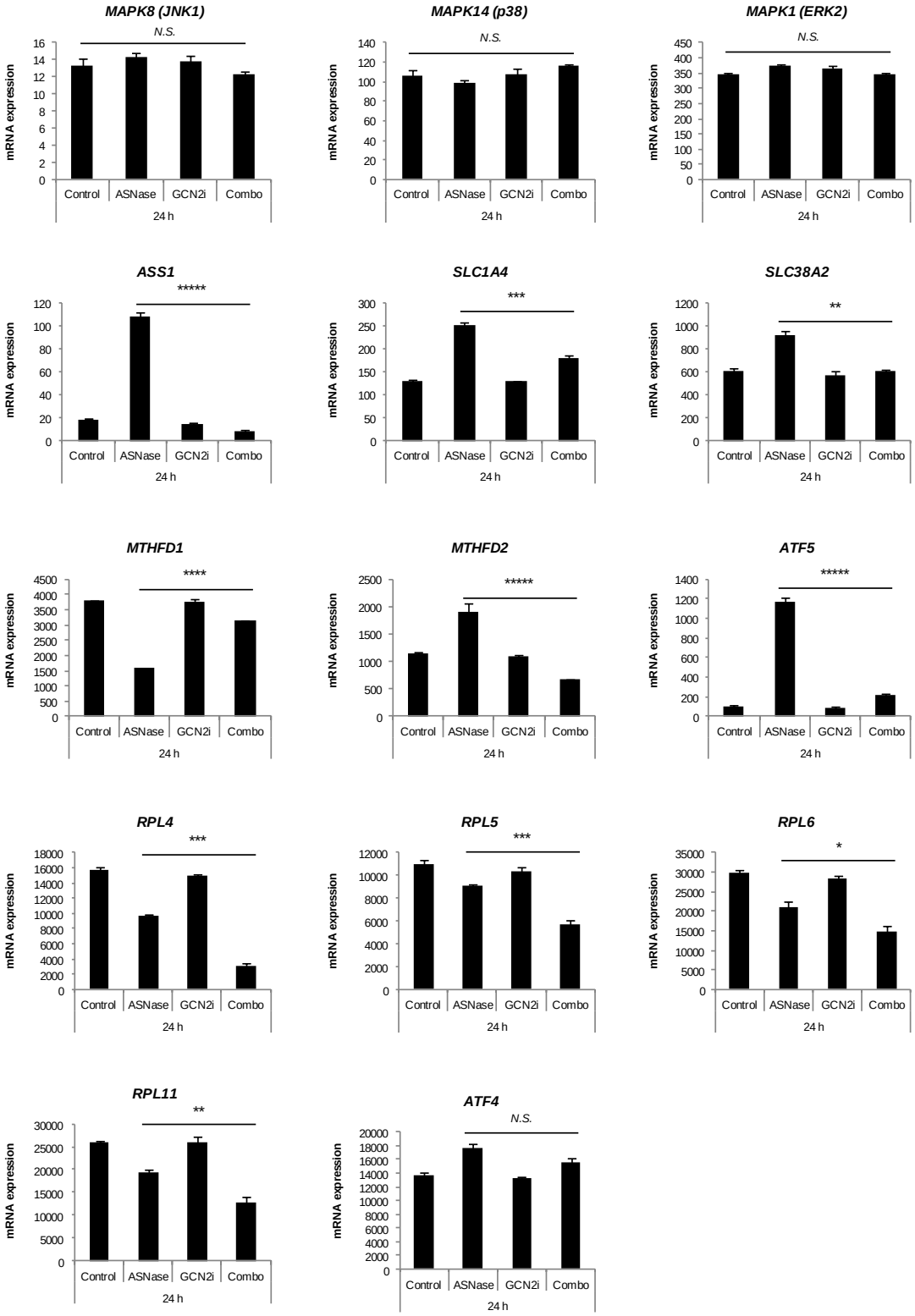

Fig. S10. Gene expression analysis of previously identified factors that determine ASNase sensitivity. CCRF-CEM cells were treated with 1 mU/mL ASNase and/or 1 μmol/L GCN2iA for 24 h, and gene expression levels were determined by microarray analysis (mean with SD; $N = 3$). *$P < 0.01$; **$P < 0.001$; ***$P < 0.0001$; ****$P < 0.00001$; *****$P < 0.000001$; and ******$P < 0.0000001$. *N.S.*, not significant ($P > 0.05$).

Supplementary Tables

Table 1. *In vitro* effects of combined treatment with ASNase and GCN2 inhibition on the proliferation of ALL cells.

ALL cell line	Log (ASNase IC_{50})			Log (ASNase IC_{70})					
	DMSO	GCN2iA	Fold change	DMSO	GCN2iA	Fold change	Log (*ASNS* mRNA)	Log (ASNS/eIF2α)	ASNase sensitivity
BALL-1	-0.35	-0.66	0.31	-0.23	-0.57	0.34	Not available	-0.29	Hyperinsensitive
CCRF-CEM	-1.78	-3.76	1.98	-1.06	-3.81	2.75	1.98	-0.92	Intermediately insensitive
CCRF-HSB-2	-3.19	-4.10	0.91	-2.26	-3.95	1.69	Not available	-0.77	Intermediately insensitive
DND-41	-3.71	-3.88	0.17	-3.68	-3.66	-0.02	1.66	-1.10	Hypersensitive
HAL-01	-0.87	-2.12	1.26	-0.30	-0.81	0.51	Not available	-0.10	Hyperinsensitive
HPB-ALL	-3.83	-3.81	-0.01	-3.72	-3.72	0.00	2.09	-1.28	Hypersensitive
Jurkat	-1.24	-3.54	2.30	-0.70	-2.76	2.06	3.06	-0.45	Intermediately insensitive
Loucy	-3.94	-3.80	-0.13	-3.76	-3.58	-0.18	1.43	-1.27	Hypersensitive
MOLT-3	-2.47	-3.95	1.48	-1.22	-3.84	2.62	Not available	-1.20	Intermediately insensitive
MOLT-4	-3.19	-3.97	0.78	-2.47	-3.79	1.33	2.10	-0.96	Intermediately insensitive
NALM-6	-0.57	-2.37	1.81	-0.10	-1.28	1.17	2.68	-0.27	Hyperinsensitive
PALL-2	-1.53	-3.39	1.86	-0.20	-2.49	2.29	Not available	-0.65	Intermediately insensitive
PEER	-3.60	-4.27	0.67	-2.72	-4.12	1.40	2.41	-0.99	Intermediately insensitive
Reh	-1.08	-3.98	2.90	-0.03	-2.68	2.65	2.63	-0.68	Intermediately insensitive
RS4;11	-3.91	-4.20	0.28	-3.76	-4.04	0.28	1.74	-1.49	Hypersensitive
SUP-B15	-4.39	-4.46	0.07	-4.29	-4.40	0.11	1.91	-1.40	Hypersensitive
SUP-T1	-0.49	-2.64	2.15	-0.02	-1.42	1.41	2.53	-0.46	Hyperinsensitive
TALL-1	-3.62	-3.63	0.00	-3.60	-3.60	0.00	2.12	-1.50	Hypersensitive
Tanoue	-0.20	-0.22	0.02	0.00	0.00	0.00	3.45	-0.09	Hyperinsensitive
TMD5	0.00	-2.85	2.85	0.00	-1.71	1.71	Not available	-1.28	Intermediately insensitive

NOTE: ALL cell lines were treated with ASNase (0.00001–1 U/mL) and/or GCN2iA (1 μmol/L). The IC_{50} or IC_{70} value of ASNase, fold change in IC_{50} or IC_{70} value after GCN2iA treatment, ASNS mRNA expression, and ASNS protein expression are shown at $\log_{10}$ scale. For ASNase sensitivity, cells are categorized as follows.

Hypersensitive; both IC_{50} and $IC_{70} < -3$ on the $\log_{10}$ scale

Intermediately insensitive; $-3 < IC_{50}$ or $IC_{70} < -1$ on the $\log_{10}$ scale

Hyperinsensitive; both IC_{50} and $IC_{70} > -1$ on the $\log_{10}$ scale

Table 2. *In vitro* effects of combined treatment with ASNase and GCN2 inhibition on the proliferation of pancreatic cancer cells.

Pancreatic cancer cell line	Log (ASNase IC_{50})				
	DMSO	GCN2iA	Fold change	Log (*ASNS* mRNA)	Log (ASNS/eIF2α)
AsPC-1	-1.08	-3.64	-2.55	3.51	-0.34
BxPC-3	-0.49	-1.02	-0.53	2.56	-0.51
Capan-1	-0.57	-0.70	-0.13	3.07	0.17
Capan-2	-0.42	-1.92	-1.50	2.56	-0.45
CFPAC-1	-0.24	-0.32	-0.09	2.96	0.13
DAN-G	-0.57	-0.69	-0.12	2.73	-0.20
HPAC	-0.74	-1.96	-1.22	2.51	-0.53
HPAF-II	-0.15	-0.33	-0.18	2.90	-0.11
HuP-T3	-0.52	-1.99	-1.47	2.45	-0.69
HuP-T4	-0.86	-2.78	-1.91	2.98	-0.51
KP4	-0.48	-0.49	-0.01	3.53	0.10
Panc 02.03	-0.69	-1.45	-0.76	2.52	-0.48
Panc 04.03	-0.51	-1.05	-0.54	3.06	-0.52
Panc 05.04	-1.88	-3.43	-1.54	2.64	-0.38
PK-45H	-0.41	-1.04	-0.62	2.50	-0.51
PK-59	-0.37	-1.66	-1.29	3.20	-0.60
SU.86.86	-1.31	-3.46	-2.15	3.55	-0.50
SUIT2	-0.92	-2.99	-2.07	2.45	-0.22
TCC-PAN2	-1.67	-3.40	-1.72	2.65	-0.45

NOTE: Pancreatic cancer cell lines were treated with ASNase (0.00001–1 U/mL) and/or 1 μmol/L GCN2iA. The IC_{50} value of ASNase, fold change in IC_{50} value after GCN2iA treatment, and mRNA and protein levels of ASNA are shown at $\log_{10}$ scale.

Supplementary References

1. Li Y, Cheng H, Zhang Z, Zhuang X, Luo J, Long H, Zhou Y, Xu Y, Taghipouran R, Li D, Patterson A, Smaill J, Tu Z, Wu D, Ren X, Ding K (2015) N-(3-Ethynyl-2,4-difluorophenyl)sulfonamide Derivatives as Selective Raf Inhibitors. *ACS Med Chem Lett* 6:543-547.
2. Nakamura A, et al. (2013) Antitumor activity of the selective pan-RAF inhibitor TAK-632 in BRAF inhibitor-resistant melanoma. *Cancer Res* 73(23):7043-7055.